Table 3. Unadjusted and Adjusted HRs for Outcomes According to Loop Diuretic Use

Outcome	n (%)		HR	95% CI	P value
	Loop diuretic use (n=1,814)	No loop diuretic use (n=491)			
All-cause death	399 (22.0%)	75 (15.3%)			
Unadjusted			1.501	1.171–1.925	0.001
Adjusted for covariates			1.545	0.986–2.420	0.058
Adjusted for matching with propensity score			1.510	1.113–2.048	0.008
Cardiac death	251 (13.8%)	41 (8.4%)			
Unadjusted			1.703	1.224–2.370	0.001
Adjusted for covariates			2.348	1.246–4.423	0.008
Adjusted for matching with propensity score			1.719	1.155–2.560	0.008
Rehospitalization	690 (38.0%)	146 (29.7%)			
Unadjusted			1.360	1.137–1.627	0.001
Adjusted for covariates			1.427	1.040–1.959	0.027
Adjusted for matching with propensity score			1.194	0.953–1.495	0.124
All-cause death or rehospitalization	834 (46.0%)	182 (37.1%)			
Unadjusted			1.326	1.129–1.558	0.001
Adjusted for covariates			1.363	1.022–1.816	0.035
Adjusted for matching with propensity score			1.236	1.010–1.511	0.040

A Cox regression model was used in the analysis adjusted for the following covariates: age, sex, eGFR at discharge, SBP at discharge, LVEF, BNP, NYHA functional class at discharge, cause of HF (ischemic, valvular), medical history (diabetes mellitus, dyslipidemia, hyperuricemia, prior myocardial infarction, and atrial fibrillation) and medication use (ACEI, β-blocker, spironolactone, thiazide, calcium-channel blocker, nitrate, statin). The same variables were used to determine the propensity score for loop diuretic use, and 465 pairs were matched. The no loop diuretic use group was the reference group.
HR, hazard ratio; CI, confidence interval. Other abbreviations as in Tables 1,2.

Results

Patients' Characteristics

The present study included 2,549 patients with a mean age of 70.7±13.3 years and 60.0% were men (**Table 1**). The causes of HF were ischemic heart disease in 32.0%, valvular heart disease in 27.7%, hypertensive heart disease in 24.2%, and dilated cardiomyopathy in 18.4%. The mean LVEF was 42.2±17.5%.

The characteristics of patients prescribed loop diuretics at discharge and those not prescribed are compared in **Table 1**. Those discharged with loop diuretics had significantly more ischemic and valvular HF etiologies; more comorbidities, such as diabetes, dyslipidemia, hyperuricemia, prior myocardial infarction, and atrial fibrillation; significantly more cases of coronary artery bypass grafting; severe HF symptoms by NYHA functional class at discharge; and SBP at discharge was significantly lower. However, diastolic blood pressure did not differ between groups. eGFR was significantly lower, and serum uric acid and plasma BNP levels were higher in patients with loop diuretics. LV end-diastolic and end-systolic diameters were significantly greater in patients with loop diuretics and LVEF tended to be lower, although this did not reach statistical significance (P=0.059).

Use of medications other than loop diuretics was compared between groups (**Table 2**). The use of ACEIs was slightly, but significantly, higher in patients with loop diuretic use (38.6% vs. 32.8%, P=0.013). However, the use of ACEI or angiotensin-receptor blocker (ARB) did not differ between groups (76.8% vs. 75.5%, P=0.511). Importantly, the combination of ACEI or ARB and β-blocker was similar between groups. However, spironolactone and nitrate were more often prescribed for the patients with loop diuretic use. On the other hand, thiazide diuretic and CCBs were more used by the patients with no loop diuretic use.

Postdischarge Clinical Outcomes According to Loop Diuretic Use

During follow-up of 2.1 years after hospital discharge, the rates of adverse outcomes were as follows: all-cause death 20.6%, cardiac death 12.7%, rehospitalization due to the worsening HF 36.3%, and all-cause death or rehospitalization 44.1%. The unadjusted rates of all-cause death, cardiac death, rehospitalization due to the worsening HF, and all-cause death or rehospitalization were significantly higher in patients with loop diuretic use (**Table 3, Figure**).

Even after adjustment for covariates in the multivariable Cox proportional hazard models, discharge use of loop diuretics, when compared to no use, was associated with an increased risk of cardiac death (HR 2.348, 95% CI 1.246–4.423, P=0.008), rehospitalization (HR 1.427, 95% CI 1.040–1.959, P=0.027), and all-cause death or rehospitalization (HR 1.363, 95% CI 1.022–1.816, P=0.035) (**Table 3**). Patients taking loop diuretics tended to have a higher risk of all-cause death, which, however, did not reach statistical significance after adjustment (P=0.058).

Furthermore, when we matched by PS, the same variables shown in **Table 1** and **Table 2** were comparable between groups. Even after adjustment for matching with PS, loop diuretic use was associated with all-cause death (HR 1.510, 95% CI 1.113–2.048, P=0.008), cardiac death (HR 1.719, 95% CI 1.155–2.560, P=0.008), and all-cause death and rehospitalization (HR 1.236, 95% CI 1.010–1.511, P=0.040). Sensitivity

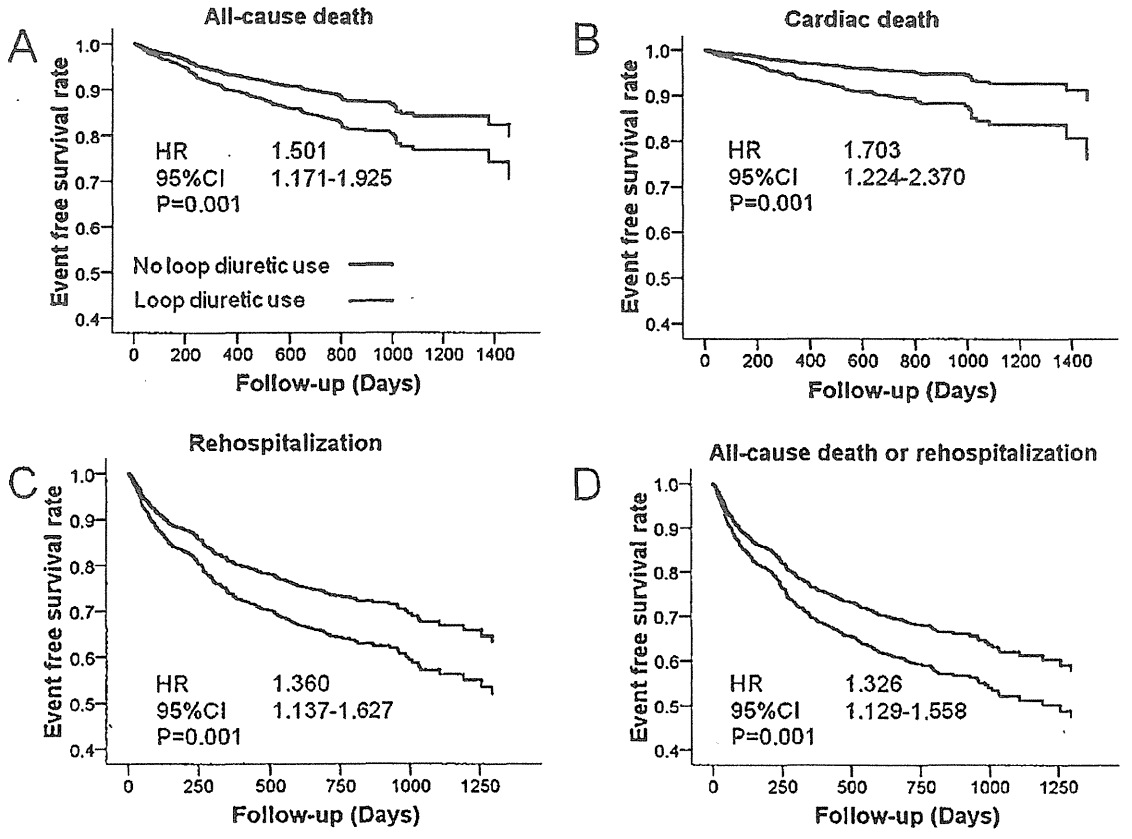

Figure. Kaplan-Meier survival curves for free from all-cause death (**A**), cardiac death (**B**), rehospitalization due to worsening heart failure (**C**), and all-cause death or rehospitalization (**D**) in hospitalized patients with loop diuretic use (red lines, n=1,814) vs. no loop diuretic use (black lines, n=491) at discharge. HR, hazard ratio; CI, confidence interval.

analysis for unmeasured confounding factors was performed. In the absence of unmeasured confounding factors, a binomial test for matched pair provides strong evidence (P=0.003) that loop diuretic use increases cardiac death, even after adjustment by PS matching. To attribute the higher rate of cardiac death to unmeasured confounding factor rather than to an effect of loop diuretic use, that unmeasured confounding factor would need to produce a 27% increase in the odds of loop diuretic use, and it would need to be a strong predictor of cardiac death.

Subgroup Analyses

The association of loop diuretic use with cardiac death was noted across a wide spectrum of HF patients (**Table 4**). Loop diuretic use was associated with increased cardiac death in HF patients who were elderly (≥70 years), with a non-ischemic etiology, no hypertension, no diabetes, and LVEF ≥40%. In any subgroup, there were no significant interactions between groups.

Discussion

The present study using the JCARE-CARD database demonstrated that among patients hospitalized with worsening HF, loop diuretic use at discharge was associated with adverse outcomes during long-term follow-up up to 2.1 years.

These findings confirm and extend the results of previous studies that suggested an association between diuretic use and worse outcomes in patients with HF.[4,7,8,22] In the SOLVD trial, use of a diuretic was associated with a 37% increase in the risk of arrhythmic death after controlling for multiple other variables of disease severity.[4] The Digitalis Investigation Group Study also found a 31% increased risk of death associated with diuretic use when using propensity matching to control for baseline differences in patients with and without diuretic use.[8] The ESCAPE trial demonstrated a linear relationship between loop diuretic dose and mortality over 6 months of follow-up in patients hospitalized with HF.[7] Moreover, in a cohort of 1,354 patients with advanced HF and reduced LVEF referred to a single center, there was a dose-dependent association between loop diuretic use and impaired survival during 2-year follow-up.[22] However, those previous studies were performed with data from patients enrolled in clinical trials or cohort studies of patients with HF and reduced LVEF, thus excluding patients with HF and preserved LVEF. In contrast, the present study included patients hospitalized due to worsening HF as the primary cause of admission independent of LVEF data. Therefore, our findings confirm the association between loop diuretic use and poor outcomes in the "real world" under current standard medical practice. Furthermore, the present results

Table 4. Subgroup Analyses of Cardiac Death According to Loop Diuretic Use

Subgroup	n	HR	95% CI	P value	P value for Interaction
Age <70 years	936	1.812	0.927–3.542	0.082	
Age ≥70 years	1,369	1.599	1.094–2.338	0.015	0.759
Male	1,376	1.604	1.042–2.471	0.032	
Female	929	1.842	1.102–3.078	0.020	0.679
Ischemic	727	1.670	0.934–2.985	0.084	
Non-Ischemic	1,578	1.691	1.131–2.528	0.010	0.975
Hypertension	1,203	1.620	0.967–2.712	0.067	
No hypertension	1,087	1.758	1.143–2.705	0.010	0.803
Diabetes	675	1.370	0.726–2.584	0.331	
No diabetes	1,626	1.826	1.239–2.690	0.002	0.443
LVEF ≥40%	1,020	2.484	1.394–4.428	0.002	
LVEF <40%	1,000	1.207	0.761–1.913	0.425	0.055

No loop diuretic use group was a reference.
Abbreviations as in Tables 1,3.

were consistent with our own previous study, in which the use of diuretics was independently associated with higher mortality in elderly patients.[9]

There are several potential mechanisms by which loop diuretics may be associated with adverse outcomes in HF patients. First, administration of diuretics to patients with HF may activate the renin-angiotensin-aldosterone system, as well as the sympathetic nervous system, both of which play a detrimental role in HF progression.[23–25] Neurohormonal activation is known to occur in patients with HF before overt symptoms appear. Plasma renin activity and norepinephrine levels have been shown to be significantly higher in HF patients with symptoms than in those without them.[25] Moreover, plasma renin activity is normal in HF patients without symptoms and who are not using diuretics and is significantly increased in patients on diuretic therapy.[25] In a tachycardia-induced animal model of HF, loop diuretic use significantly accelerated LV systolic dysfunction, elevated the serum aldosterone level, and increased basal sodium-calcium exchanger currents.[6] Activation of the renin-angiotensin-aldosterone system induces myocardial fibrosis, oxidative stress, stimulation of proinflammatory cytokines, and myocardial fibrosis.[26–29] Second, loop diuretics may also decrease intravascular volume and the GFR, which may also be caused by neurohormonal activation. Previous studies, including our own, have demonstrated that renal dysfunction is a common and independent risk for cardiovascular adverse outcomes in HF patients.[11,30–39] Finally, loop diuretics cause electrolyte imbalances, such as decreases in potassium and magnesium,[40,41] which may increase the risk of fatal arrhythmias and sudden cardiac death.[40–44]

Clinical Implications

Based on findings suggesting an association between diuretic use and worsening outcomes in patients with HF, guidelines from the European Society of Cardiology recommend that diuretics be used for HF patients with clinical symptoms or signs of volume overload and congestion.[45] The practice guideline from the Heart Failure Society of America also recommends loop diuretics at doses needed to produce diuresis sufficient to achieve an optimal volume status.[46] Therefore, routine chronic use of loop diuretics for HF patients without fluid retention needs to be avoided.

Study Limitations

Several limitations inherent in the design of the registry should be considered. First, the documentation of loop diuretic use at hospital discharge might not accurately reflect continuation over time or start after discharge. Moreover, we did not collect information regarding the dose and type of loop diuretic, such as furosemide and torsemide, and whether loop diuretics were initiated during or before hospitalization. Therefore, we could not assess the dose-effect relation in the study patients. However, higher doses are associated with higher mortality, based on the results of the ESCAPE trial.[7] Second, information regarding the serum electrolyte concentration was not obtained in this database, so we could not assess the impact of hypokalemia, hyponatremia, and hypomagnesemia on outcomes. Third, the present study was not a prospective randomized trial and, despite covariate adjustment and adjustment for matching by PS and sensitivity analysis, other measured and unmeasured factors may have influenced the outcomes. Renal dysfunction, hyperuricemia and electrolyte imbalances commonly associated with loop diuretic use might affect the outcomes. Specifically, patients who received loop diuretics might do so because of greater disease severity compared to those who did not. However, the present study demonstrated an adverse effect of loop diuretics, even after extensive multivariable adjustment of other known predictors and adjustment for PS matching, and it was consistent among the different subgroups studied. Moreover, this has been persistently reported in most prior studies.[4,7,8,22] Even though the present finding that use of loop diuretics was associated with worse outcomes is consistent with similar previous reports, unmeasured or unanalyzed factors that motivated the physicians caring for HF patients to give loop diuretics could have also put these patients at higher risk for death and subsequent hospitalization. It is difficult, even impossible, to account for these factors and the conclusion of the present study could be considered as "hypothesis generating". Finally, data were dependent on the accuracy of documentation and abstraction by the individual medical centers that participated in this study.

Conclusions

Among patients hospitalized with worsening HF, loop diuretic use at discharge was associated with adverse outcomes during a long-term follow-up of up to 2.1 years. The potential risk of

loop diuretics for the larger numbers of HF patients encountered in routine clinical practice was suggested.

Acknowledgments

The JCARE-CARD investigators and participating cardiologists are listed in the Appendix of our previous publication.[10] This study could not have been carried out without the help, cooperation and support of the cardiologists in the survey institutions. We thank them for allowing us to obtain the data. The JCARE-CARD was supported by the Japanese Circulation Society and the Japanese Society of Heart Failure and by grants from Health Sciences Research Grants from the Japanese Ministry of Health, Labor and Welfare (Comprehensive Research on Cardiovascular Diseases), the Japan Heart Foundation, and Japan Arteriosclerosis Prevention Fund.

References

1. Hunt SA. ACC/AHA 2005 guideline update for the diagnosis and management of chronic heart failure in the adult: A report of the American College of Cardiology/American Heart Association Task Force on Practice Guidelines (Writing Committee to Update the 2001 Guidelines for the Evaluation and Management of Heart Failure). *J Am Coll Cardiol* 2005; **46:** e1–e82.
2. Jessup M, Abraham WT, Casey DE, Feldman AM, Francis GS, Ganiats TG, et al. 2009 focused update: ACCF/AHA Guidelines for the Diagnosis and Management of Heart Failure in Adults: A report of the American College of Cardiology Foundation/American Heart Association Task Force on Practice Guidelines: Developed in collaboration with the International Society for Heart and Lung Transplantation. *Circulation* 2009; **119:** 1977–2016.
3. Francis GS, Siegel RM, Goldsmith SR, Olivari MT, Levine TB, Cohn JN. Acute vasoconstrictor response to intravenous furosemide in patients with chronic congestive heart failure: Activation of the neurohumoral axis. *Ann Intern Med* 1985; **103:** 1–6.
4. Cooper HA, Dries DL, Davis CE, Shen YL, Domanski MJ. Diuretics and risk of arrhythmic death in patients with left ventricular dysfunction. *Circulation* 1999; **100:** 1311–1315.
5. Lopez B, Querejeta R, Gonzalez A, Sanchez E, Larman M, Diez J. Effects of loop diuretics on myocardial fibrosis and collagen type I turnover in chronic heart failure. *J Am Coll Cardiol* 2004; **43:** 2028–2035.
6. McCurley JM, Hanlon SU, Wei SK, Wedam EF, Michalski M, Haigney MC. Furosemide and the progression of left ventricular dysfunction in experimental heart failure. *J Am Coll Cardiol* 2004; **44:** 1301–1307.
7. Hasselblad V, Gattis Stough W, Shah MR, Lokhnygina Y, O'Connor CM, Califf RM, et al. Relation between dose of loop diuretics and outcomes in a heart failure population: Results of the ESCAPE trial. *Eur J Heart Fail* 2007; **9:** 1064–1069.
8. Ahmed A, Husain A, Love TE, Gambassi G, Dell'Italia LJ, Francis GS, et al. Heart failure, chronic diuretic use, and increase in mortality and hospitalization: An observational study using propensity score methods. *Eur Heart J* 2006; **27:** 1431–1439.
9. Hamaguchi S, Kinugawa S, Goto D, Tsuchihashi-Makaya M, Yokota T, Yamada S, et al. Predictors of long-term adverse outcomes in elderly patients over 80 years hospitalized with heart failure. *Circ J* 2011; **75:** 2403–2410.
10. Tsutsui H, Tsuchihashi-Makaya M, Kinugawa S, Goto D, Takeshita A. Clinical characteristics and outcome of hospitalized patients with heart failure in Japan. *Circ J* 2006; **70:** 1617–1623.
11. Hamaguchi S, Tsuchihashi-Makaya M, Kinugawa S, Yokota T, Ide T, Takeshita A, et al. Chronic kidney disease as an independent risk for long-term adverse outcomes in patients hospitalized with heart failure in Japan: Report from the Japanese Cardiac Registry of Heart Failure in Cardiology (JCARE-CARD). *Circ J* 2009; **73:** 1442–1447.
12. Hamaguchi S, Tsuchihashi-Makaya M, Kinugawa S, Yokota T, Takeshita A, Yokoshiki H, et al. Anemia is an independent predictor of long-term adverse outcomes in patients hospitalized with heart failure in Japan: A report from the Japanese Cardiac Registry of Heart Failure in Cardiology (JCARE-CARD). *Circ J* 2009; **73:** 1901–1908.
13. Hamaguchi S, Yokoshiki H, Kinugawa S, Tsuchihashi-Makaya M, Yokota T, Takeshita A, et al. Effects of atrial fibrillation on long-term outcomes in patients hospitalized for heart failure in Japan: A report from the Japanese Cardiac Registry of Heart Failure in Cardiology (JCARE-CARD). *Circ J* 2009; **73:** 2084–2090.
14. Tsuchihashi-Makaya M, Hamaguchi S, Kinugawa S, Yokota T, Goto D, Yokoshiki H, et al. Characteristics and outcomes of hospitalized patients with heart failure and reduced vs preserved ejection fraction: Report from the Japanese Cardiac Registry of Heart Failure in Cardiology (JCARE-CARD). *Circ J* 2009; **73:** 1893–1900.
15. Hamaguchi S, Kinugawa S, Tsuchihashi-Makaya M, Goto K, Goto D, Yokota T, et al. Spironolactone use at discharge was associated with improved survival in hospitalized patients with systolic heart failure. *Am Heart J* 2010; **160:** 1156–1162.
16. Hamaguchi S, Tsuchihashi-Makaya M, Kinugawa S, Goto D, Yokota T, Goto K, et al. Body mass index is an independent predictor of long-term outcomes in patients hospitalized with heart failure in Japan. *Circ J* 2010; **74:** 2605–2611.
17. Tsuchihashi-Makaya M, Furumoto T, Kinugawa S, Hamaguchi S, Goto K, Goto D, et al. Discharge use of angiotensin receptor blockers provides comparable effects with angiotensin-converting enzyme inhibitors on outcomes in patients hospitalized for heart failure. *Hypertens Res* 2010; **33:** 197–202.
18. Tsuchihashi-Makaya M, Kinugawa S, Yokoshiki H, Hamaguchi S, Yokota T, Goto D, et al. Beta-blocker use at discharge in patients hospitalized for heart failure is associated with improved survival. *Circ J* 2010; **74:** 1364–1371.
19. Hamaguchi S, Furumoto T, Tsuchihashi-Makaya M, Goto K, Goto D, Yokota T, et al. Hyperuricemia predicts adverse outcomes in patients with heart failure. *Int J Cardiol* 2011; **151:** 143–147.
20. Tsuchihashi-Makaya M, Hamaguchi S, Kinugawa S, Goto K, Goto D, Furumoto T, et al. Sex differences with respect to clinical characteristics, treatment, and long-term outcomes in patients with heart failure. *Int J Cardiol* 2011; **150:** 338–339.
21. Rosenbaum PR. Sensitivity to hidden bias. *In*: Rosenbaum PR, editor. Observational studies. 2nd edn. New York: Springer; 2002; 110–124.
22. Eshaghian S, Horwich TB, Fonarow GC. Relation of loop diuretic dose to mortality in advanced heart failure. *Am J Cardiol* 2006; **97:** 1759–1764.
23. Dzau VJ, Colucci WS, Hollenberg NK, Williams GH. Relation of the renin-angiotensin-aldosterone system to clinical state in congestive heart failure. *Circulation* 1981; **63:** 645–651.
24. Packer M. The neurohormonal hypothesis: A theory to explain the mechanism of disease progression in heart failure. *J Am Coll Cardiol* 1992; **20:** 248–254.
25. Francis GS, Benedict C, Johnstone DE, Kirlin PC, Nicklas J, Liang CS, et al. Comparison of neuroendocrine activation in patients with left ventricular dysfunction with and without congestive heart failure: A substudy of the Studies of Left Ventricular Dysfunction (SOLVD). *Circulation* 1990; **82:** 1724–1729.
26. Weber KT, Brilla CG. Pathological hypertrophy and cardiac interstitium: Fibrosis and renin-angiotensin-aldosterone system. *Circulation* 1991; **83:** 1849–1865.
27. Lijnen P, Petrov V. Induction of cardiac fibrosis by aldosterone. *J Mol Cell Cardiol* 2000; **32:** 865–879.
28. Oudit GY, Kassiri Z, Patel MP, Chappell M, Butany J, Backx PH, et al. Angiotensin II-mediated oxidative stress and inflammation mediate the age-dependent cardiomyopathy in ACE2 null mice. *Cardiovasc Res* 2007; **75:** 29–39.
29. Lopez B, Gonzalez A, Diez J. Circulating biomarkers of collagen metabolism in cardiac diseases. *Circulation* 2010; **121:** 1645–1654.
30. Tokmakova MP, Skali H, Kenchaiah S, Braunwald E, Rouleau JL, Packer M, et al. Chronic kidney disease, cardiovascular risk, and response to angiotensin-converting enzyme inhibition after myocardial infarction: The Survival And Ventricular Enlargement (SAVE) study. *Circulation* 2004; **110:** 3667–3673.
31. Shlipak MG, Smith GL, Rathore SS, Massie BM, Krumholz HM. Renal function, digoxin therapy, and heart failure outcomes: Evidence from the digoxin intervention group trial. *J Am Soc Nephrol* 2004; **15:** 2195–2203.
32. McAlister FA, Ezekowitz J, Tonelli M, Armstrong PW. Renal insufficiency and heart failure: Prognostic and therapeutic implications from a prospective cohort study. *Circulation* 2004; **109:** 1004–1009.
33. Hillege HL, Nitsch D, Pfeffer MA, Swedberg K, McMurray JJ, Yusuf S, et al. Renal function as a predictor of outcome in a broad spectrum of patients with heart failure. *Circulation* 2006; **113:** 671–678.
34. Smith GL, Lichtman JH, Bracken MB, Shlipak MG, Phillips CO, DiCapua P, et al. Renal impairment and outcomes in heart failure: Systematic review and meta-analysis. *J Am Coll Cardiol* 2006; **47:** 1987–1996.
35. Go AS, Yang J, Ackerson LM, Lepper K, Robbins S, Massie BM, et al. Hemoglobin level, chronic kidney disease, and the risks of death and hospitalization in adults with chronic heart failure: The Anemia in Chronic Heart Failure: Outcomes and Resource Utilization (ANCHOR) Study. *Circulation* 2006; **113:** 2713–2723.
36. Heywood JT, Fonarow GC, Costanzo MR, Mathur VS, Wigneswaran JR, Wynne J. High prevalence of renal dysfunction and its impact on outcome in 118,465 patients hospitalized with acute decompensated

heart failure: A report from the ADHERE database. *J Card Fail* 2007; **13:** 422–430.
37. Komukai K, Ogawa T, Yagi H, Date T, Sakamoto H, Kanzaki Y, et al. Decreased renal function as an independent predictor of re-hospitalization for congestive heart failure. *Circ J* 2008; **72:** 1152–1157.
38. Shiba N, Matsuki M, Takahashi J, Tada T, Watanabe J, Shimokawa H. Prognostic importance of chronic kidney disease in Japanese patients with chronic heart failure. *Circ J* 2008; **72:** 173–178.
39. Vaz Perez A, Otawa K, Zimmermann AV, Stockburger M, Muller-Werdan U, Werdan K, et al. The impact of impaired renal function on mortality in patients with acutely decompensated chronic heart failure. *Eur J Heart Fail* 2010; **12:** 122–128.
40. Robertson JI. Diuretics, potassium depletion and the risk of arrhythmias. *Eur Heart J* 1984; 5(Suppl A): 25–28.
41. Hollifield JW. Potassium and magnesium abnormalities: Diuretics and arrhythmias in hypertension. *Am J Med* 1984; **77:** 28–32.
42. Dyckner T. Relation of cardiovascular disease to potassium and magnesium deficiencies. *Am J Cardiol* 1990; **65:** 44K–46K.
43. Dyckner T, Wester PO. Potassium/magnesium depletion in patients with cardiovascular disease. *Am J Med* 1987; **82:** 11–17.
44. Kjeldsen K. Hypokalemia and sudden cardiac death. *Exp Clin Cardiol* 2010; **15:** e96–e99.
45. Dickstein K, Cohen-Solal A, Filippatos G, McMurray JJ, Ponikowski P, Poole-Wilson PA, et al. ESC Guidelines for the diagnosis and treatment of acute and chronic heart failure 2008: The Task Force for the Diagnosis and Treatment of Acute and Chronic Heart Failure 2008 of the European Society of Cardiology. Developed in collaboration with the Heart Failure Association of the ESC (HFA) and endorsed by the European Society of Intensive Care Medicine (ESICM). *Eur Heart J* 2008; **29:** 2388–2442.
46. America HFSO. Disease management in heart failure. *J Card Fail* 2006; **12:** e58–e69.

Circulation Research
JOURNAL OF THE AMERICAN HEART ASSOCIATION

American Heart Association®

Activation of Natural Killer T Cells Ameliorates Postinfarct Cardiac Remodeling and Failure in MiceNovelty and Significance

Mochamad Ali Sobirin, Shintaro Kinugawa, Masashige Takahashi, Arata Fukushima, Tsuneaki Homma, Taisuke Ono, Kagami Hirabayashi, Tadashi Suga, Putri Azalia, Shingo Takada, Masaru Taniguchi, Toshinori Nakayama, Naoki Ishimori, Kazuya Iwabuchi and Hiroyuki Tsutsui

Circ Res. 2012;111:1037-1047; originally published online August 10, 2012;
doi: 10.1161/CIRCRESAHA.112.270132
Circulation Research is published by the American Heart Association, 7272 Greenville Avenue, Dallas, TX 75231

Print ISSN: 0009-7330. Online ISSN: 1524-4571

Activation of Natural Killer T Cells Ameliorates Postinfarct Cardiac Remodeling and Failure in Mice

Mochamad Ali Sobirin, Shintaro Kinugawa, Masashige Takahashi, Arata Fukushima, Tsuneaki Homma, Taisuke Ono, Kagami Hirabayashi, Tadashi Suga, Putri Azalia, Shingo Takada, Masaru Taniguchi, Toshinori Nakayama, Naoki Ishimori, Kazuya Iwabuchi, Hiroyuki Tsutsui

Rationale: **Chronic inflammation in the myocardium is involved in the development of left ventricular (LV) remodeling and failure after myocardial infarction (MI). Invariant natural killer T (iNKT) cells have been shown to produce inflammatory cytokines and orchestrate tissue inflammation. However, no previous studies have determined the pathophysiological role of iNKT cells in post-MI LV remodeling.**

Objective: **The purpose of this study was to examine whether the activation of iNKT cells might affect the development of LV remodeling and failure.**

Methods and Results: **After creation of MI, mice received the injection of either α-galactosylceramide (αGC; n=27), the activator of iNKT cells, or phosphate-buffered saline (n=31) 1 and 4 days after surgery, and were followed during 28 days. Survival rate was significantly higher in MI+αGC than MI+PBS (59% versus 32%, $P<0.05$). LV cavity dilatation and dysfunction were significantly attenuated in MI+αGC, despite comparable infarct size, accompanied by a decrease in myocyte hypertrophy, interstitial fibrosis, and apoptosis. The infiltration of iNKT cells were increased during early phase in noninfarcted LV from MI and αGC further enhanced them. It also enhanced LV interleukin (IL)-10 gene expression at 7 days, which persisted until 28 days. AntienIL-10 receptor antibody abrogated these protective effects of αGC on MI remodeling. The administration of αGC into iNKT cell-deficient $J\alpha18^{-/-}$ mice had no such effects, suggesting that αGC was a specific activator of iNKT cells.**

Conclusions: **iNKT cells play a protective role against post-MI LV remodeling and failure through the enhanced expression of cardioprotective cytokines such as IL-10. (*Circ Res.* 2012; 111:1037-1047.)**

Key Words: natural killer T cells ■ myocardial infarction ■ inflammation ■ heart failure ■ cytokines

Myocardial infarction (MI) leads to the development of heart failure (HF), which is the major cause of death in post-MI patients. The changes in left ventricular (LV) geometry, such as cavity dilatation associated with myocyte hypertrophy and interstitial fibrosis, referred to as remodeling, contribute to the development of depressed cardiac function in HF after MI.[1] It has been reported that monocytes and lymphocytes are infiltrated in noninfarcted area as well as infarcted area of LV after MI.[2,3] Chemokines, monocyte chemoattractant protein-1 (MCP-1), and RANTES (regulated on activation normally T-cell expressed and secreted), are essential factors in the recruitment and activation of monocyte and lymphocyte. These chemokines are also increased in noninfarcted LV after MI and contribute to local inflammation through the release of inflammatory cytokines including tumor necrosis factor-α (TNF-α).[2,4] Targeted deletion of CC chemokine receptor 2 or anti–MCP-1 gene therapy has been shown to attenuate LV remodeling after MI.[2,5] Thus, chronic tissue inflammation plays an important role in LV remodeling process.

Invariant natural killer T (iNKT) cells are innate-like T-lymphocyte population coexpressing NK markers and an αβ T-cell receptor that recognize glycolipid antigens. They can rapidly and robustly produce a mixture of T-helper type 1 (T_H1) and T_H2 cytokines, such as TNF-α, interferon-γ (IFN-γ), interleukin (IL)-10, and IL-4, and also a vast array of chemokines in shaping subsequent adaptive immune response.[6] Thus, iNKT cells can function as a bridge between the innate and adaptive immune systems, and orchestrate

Original received March 25, 2012; revision received August 8, 2012; accepted August 10, 2012. In July 2012, the average time from submission to first decision for all original research papers submitted to *Circulation Research* was 11.2 days.

From the Department of Cardiovascular Medicine, Hokkaido University Graduate School of Medicine, Sapporo Faculty of Medicine, Sapporo, Japan (M.A.S., S.K., M.T., A.F., T.H., T.O., K.H., T.S., P.A., S.T., N.I., H.T.); Diponegoro University, Semarang, Indonesia (M.A.S.); RIKEN Research Center for Allergy and Immunology, Kanagawa, Japan (M.T.); the Department of Immunology, Graduate School of Medicine, Chiba University, Chiba, Japan (T.N.); and the Division of Immunobiology, Kitasato University School of Medicine, Kanagawa, Japan (K.I.).

The online-only Data Supplement is available with this article at http://circres.ahajournals.org/lookup/suppl/doi:10.1161/CIRCRESAHA.112.270132/-/DC1.

Correspondence to Shintaro Kinugawa, MD, PhD, Department of Cardiovascular Medicine, Hokkaido University Graduate School of Medicine, Kita-15, Nishi-7, Kita-ku, Sapporo 060–8638, Japan. E-mail tuckahoe@med.hokudai.ac.jp

Circulation Research **is available at http://circres.ahajournals.org** **DOI: 10.1161/CIRCRESAHA.112.270132**

Non-standard Abbreviations and Acronyms	
αGC	α-galactosylceramide
HF	heart failure
IFN-γ	interferon-γ
IL	interleukin
iNKT	invariant natural killer T
LV	left ventricle
MCP-1	monocyte chemoattractant protein-1
MI	myocardial infarction
MMP	matrix metalloproteinase
NK	natural killer
PBS	phosphate-buffered saline
qRT-PCR	quantitative reverse transcriptase–polymerase chain reaction
RANTES	regulated on activation normally T cell expressed and secreted
T_H1	T-helper type 1
T_H2	T-helper type 2
TNF-α	tumor necrosis factor-α

tissue inflammation. Indeed, we have shown that iNKT cells activate vascular wall inflammation in atherogenesis and adipose tissue inflammation in obesity-induced glucose intolerance.[7,8] On the other hand, iNKT cells play a protective role against autoimmune and inflammatory diseases such as type 1 diabetes,[9,10] allergic encephalomyelitis,[9,11] and rheumatoid arthritis.[12] These findings suggest that iNKT cells may have bidirectional effects on tissue inflammation. However, no previous studies have examined the changes of iNKT cells and their pathophysiological role in LV remodeling and failure after MI.

Therefore, the purpose of the present study was to determine whether iNKT cells might affect the development of LV remodeling and failure after MI. We demonstrated that the activation of iNKT cells by α-galactosylceramide (αGC), a specific activator for iNKT cells,[13] attenuated the development of LV remodeling and failure after MI in mice. The enhanced gene expression of IL-10 might be involved in these beneficial effects of iNKT cells on this disease process.

Methods

All procedures and animal care were approved by our institutional animal research committee and conformed to the animal care guideline for the Care and Use of Laboratory Animals in Hokkaido University Graduate School of Medicine.

Experiment 1: Time-Dependent Changes of iNKT Cell Receptors in Post-MI Hearts

Animal Models

MI was created in male C57BL/6J mice, 6 to 8 weeks old and 20 to 25 g body weight, by ligating the left coronary artery as described previously.[14] Sham operation without ligating the coronary artery was also performed as control. MI mice were euthanized and the hearts were excised at days 3, 7, 14, and 28 for quantitative reverse transcriptase–polymerase chain reaction (qRT-PCR) measurements.

Quantitative RT-PCR

Quantitative PCR for Vα14Jα18 (a specific marker of iNKT cells) was performed, as described previously.[8]

Experiment 2: Effects of iNKT Cell Activation on Post-MI Heart Animal Models

Sham and MI mice were created in male C57BL/6J as described in experiment 1. Each group of mice was randomly divided into 2 groups; either αGC (0.1 μg/g body weight; Funakoshi Company, Ltd, Tokyo, Japan), the activator of iNKT cells, or phosphate-buffered saline (PBS) was administered via intraperitoneal injection 1 and 4 days after surgery. The concentration of αGC was chosen based on the previous study of its efficacy.[8] Thus, the experiment was performed in the following 4 groups of mice; sham+PBS (n=10), sham+αGC (n=10), MI+PBS (n=31), and MI+αGC (n=27).

Survival

The survival analysis was performed in all 4 groups of mice. During the study period, the cages were inspected daily for dead animals. All dead mice were examined for the presence of MI as well as pleural effusion and cardiac rupture.

Echocardiographic and Hemodynamic Measurements

Echocardiographic and hemodynamic measurements were performed under light anesthesia with tribromoethanol/amylene hydrate (avertin; 2.5% wt/vol, 8 μL/g ip), as described previously.[14]

Myocardial Histopathology, Infarct Size, Myocardial Apoptosis, and Matrix Metalloproteinase Zymography

Myocyte cross-sectional area, collagen volume fraction, infarct size, myocardial apoptosis, and zymographic matrix metalloproteinase (MMP) levels were determined as described previously.[14,15]

Isolation of Cardiac Mononuclear Cell and Flow Cytometry

Cardiac mononuclear cells from 3 mice were isolated, pooled, and subjected to flow cytometric analysis as previously described.[7,16]

Quantitative RT-PCR

Quantitative PCR for Vα14Jα18, CD11c (a marker of M1 macrophages), arginase-1 (a marker of M2 macrophages), MCP-1, RANTES, IFN-γ, IL-4, IL-6, TNF-α, and IL-10 was performed, as described previously.[8]

Immunohistochemistry

LV sections were immunostained with antibody against mouse MAC3 (a macrophage marker), mouse CD3 (a T-cell marker), or mouse myeloperoxidase (a leukocyte marker), followed by counterstaining with hematoxylin.

Plasma Cytokine Concentration

Plasma IL-10, TNF-α, IFN-γ, IL-6, and IL-4 levels were measured by commercially available ELISA kit (R&D systems, Inc) in all groups.

Experiment 3: Effects of IL-10 Neutralization on αGC-Treated Post-MI Hearts

MI mice were divided into the following 3 groups; MI+αGC (n=18), MI+anti–IL-10 receptor antibody (n=12), and MI+αGC+anti–IL-10 receptor antibody (n=19). αGC was administered identically as in experiment 2. Anti–IL-10 receptor antibody (500 μg/mouse, BD Pharmingen, San Diego, CA) was administered via

intraperitoneal injection 1, 4, and 14 days after surgery. The concentration of anti–IL-10 receptor antibody was chosen based on the previous study of its efficacy.[12] Four weeks after surgery, echocardiographic and hemodynamic measurements were performed. Separate groups of mice were used in the MI+αGC group in experiment 2.

Experiment 4: Specificity of αGC for NKT Cells

Vα14⁺ NKT cell-deficient Jα18$^{-/-}$ (Jα18 KO) mice were provided by Dr M. Taniguchi (RIKEN, Yokohama, Japan) and back-crossed 10 times to C57BL/6J.[17] Sham and MI mice were created in male Jα18 KO mice as described in experiment 1. Each group of mice was treated identically to experiment 2. Thus, the experiment was performed in the following 4 groups; KO+sham+PBS, KO+sham+αGC, KO+MI+PBS, and KO+MI+αGC. One week after surgery, all mice (n=9 for each group) were euthanized and used for immunohistochemistry (n=3 for each group) and for qRT-PCR (n=6 for each group). These analyses were performed as described in experiment 2.

Statistical Analysis

Data are expressed as mean±SEM. Survival analysis was performed by the Kaplan-Meier method, and between-group differences in survival were tested by the log-rank test. A between-group comparison of means was performed by 1-way ANOVA, followed by *t* test. The Bonferroni correction was applied for multiple comparisons of means. $P<0.05$ was considered statistically significant.

The authors had full access to and take full responsibility for the integrity of the data. All authors had read and agreed to the manuscript as written.

Results

Experiment 1: Time-Dependent Changes of iNKT Cell Receptors in Post-MI Hearts

The quantification of iNKT cells by Vα14/Jα18 gene expression demonstrated that iNKT cell infiltration into the noninfarcted LV was significantly enhanced at 7 days (1.7±0.2-fold changes from baseline, $P<0.05$ versus baseline) after MI and returned to baseline at 14 and 28 days after MI (1.0±0.2- and 1.1±0.1-fold changes from baseline, respectively). In the infarcted LV, its gene expression was significantly elevated 7 days and remained elevated 28 days after MI (data not shown).

Experiment 2: Effects of iNKT Cell Activation on Post-MI Hearts

By using flow cytometric analysis, iNKT cells were detected in LV from all groups of mice (Figure 1A). αGC injection increased iNKT cells infiltration into the noninfarcted LV both in sham+αGC and MI+αGC mice after 7 days (Figure 1A). Moreover, it remained enhanced at 28 days in MI+αGC (Figure 1A).

Quantitative RT-PCR also demonstrated that gene expression of Vα14/Jα18, a marker of iNKT cell infiltration, was significantly elevated in the noninfarcted LV from sham+αGC and MI+αGC mice after 7 days (Figure 1B). Interestingly, it remained significantly increased at 28 days only in MI+αGC (Figure 1B).

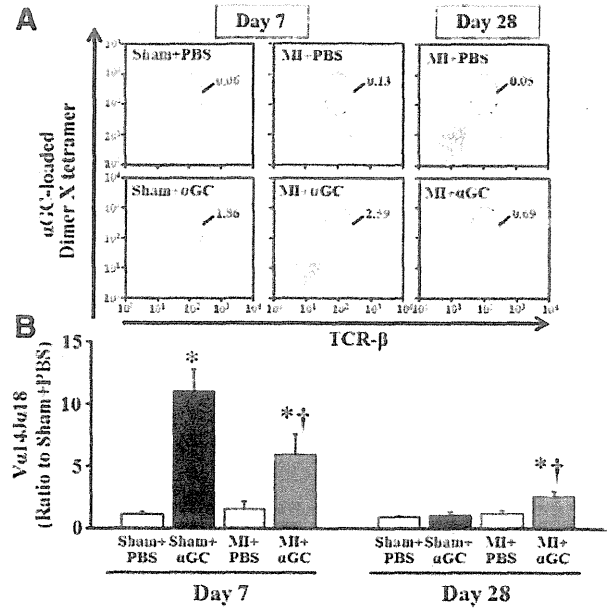

Figure 1. A, Representative flow cytometric assessment of cardiac mononuclear cells obtained from sham+PBS, sham+αGC, MI+PBS, and MI+αGC at days 7 and 28. Cardiac mononuclear cells from 5 different mice for each group were pooled and analyzed. The experiments were performed 3 times. iNKT cells were gated as the αGC-loaded dimer X tetramer⁺TCR-β⁺ population. The **inset** numbers are a percentage of the gated region of the samples. **B**, Gene expression of Vα14/Jα18 in noninfarcted LV from sham+PBS, sham+αGC, MI+PBS, and MI+αGC 7 days (n=6) and 28 days (n=4) after surgery. They were normalized to GAPDH gene expression and expressed as ratio to sham+PBS values. Data are expressed as mean±SEM. *$P<0.05$ versus sham+PBS, †$P<0.05$ versus MI+PBS.

Survival

There were no deaths in sham-operated groups. The survival rate during 28 days was significantly higher in MI+αGC compared with MI+PBS mice (59% versus 32%; $P<0.05$; Figure 2A). Thirteen MI+PBS (42%) and 8 MI+αGC (30%) mice died of LV rupture (*P*=NS).

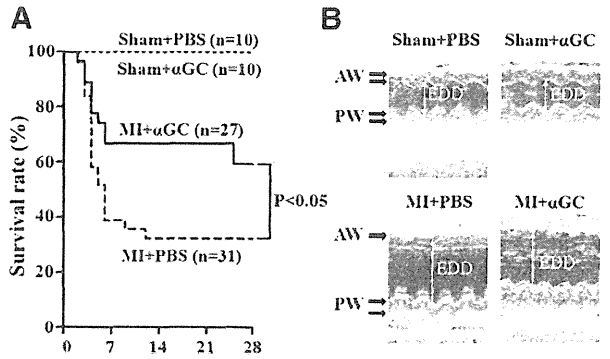

Figure 2. A, Percent survival of sham+PBS (n=10), sham+αGC (n=10), MI+PBS (n=31), and MI+αGC (n=27) mice shown by Kaplan-Meier method. B, Representative M-mode echocardiographic images obtained from sham+PBS, sham+αGC, MI+PBS, and MI+αGC. AW indicates anterior wall; PW, posterior wall; EDD, end-diastolic diameter.

Table 1. Echocardiography, Hemodynamics, and Organ Weights in Experiment 2

	Sham+PBS (n=10)	Sham+αGC (n=10)	MI+PBS (n=10)	MI+αGC (n=16)
Echocardiography				
Heart rate, bpm	522±10	522±12	531±16	520±13
LVEDD, mm	3.4±0.1	3.4±0.04	5.4±0.1*	5.0±0.1*†
LVESD, mm	2.1±0.03	2.1±0.04	4.5±0.1*	4.1±0.1*†
FS, %	38.2±0.7	38.3±0.6	16.5±0.6*	18.8±0.6*†
AWT, mm	0.63±0.01	0.62±0.01	0.31±0.01*	0.30±0.01*
PWT, mm	0.68±0.02	0.68±0.01	0.97±0.01*	0.96±0.02*
Hemodynamics				
Heart rate, min	507±9	499±9	485±23	495±11
Mean AoP, mm Hg	78.1±2	77.7±2	75.0±3	79.3±1
LVEDP, mm Hg	1.7±0.3	2.3±0.1	10.7±1.1*	6.6±0.6*†
LV +dP/dt, mm Hg/s	15 625±623	14 972±398	7352±697*	9386±476*†
LV −dP/dt, mm Hg/s	9983±697	9130±691	5045±482*	5861±286*
Organ weights				
Body wt, g	25.1±0.3	24.9±0.2	24.5±0.4	24.8±0.3
Heart wt/body wt, mg/g	4.6±0.1	4.5±0.1	6.8±0.2*	6.1±0.1*†
Lung wt/body wt, mg/g	5.2±0.03	5.2±0.1	7.2±0.7*	5.9±0.2†
Infarct size, %	...	...	56±2	55±1

LVEDD indicates left ventricular end-diastolic diameter; LVESD, left ventricular end-systolic diameter; FS, fractional shortening; AWT, anterior wall thickness; PWT, posterior wall thickness; AoP, aortic pressure; LVEDP, left ventricular end-diastolic pressure; wt, weight. Data are mean±SEM.

*$P<0.05$ versus sham+PBS.

†$P<0.05$ versus MI+PBS.

Echocardiography and Hemodynamics

The echocardiographic and hemodynamic data from 4 groups of survived mice at 28 days are shown in Figure 2B and Table 1. There were no significant differences in either echocardiographic or hemodynamic parameters between sham+PBS and sham+αGC mice. LV diameters were significantly greater and LV fractional shortening was significantly lower in MI mice than sham mice. These changes were ameliorated by the treatment of MI mice with αGC. There were no significant differences in heart rate or aortic blood pressure among groups. LV end-diastolic pressure (LVEDP) was significantly increased, and LV +dP/dt and LV −dP/dt were significantly decreased in MI compared with sham, which was ameliorated by the treatment of MI mice with αGC.

Organ Weights, Infarct Size, and Histology

There were no significant differences in heart weight/body weight and lung weight/body weight between sham+PBS and sham+αGC mice (Table 1). In agreement with LVEDP, heart weight/body weight and lung weight/body weight were increased in MI mice, and these increases were significantly attenuated in MI+αGC (Table 1).

Infarct size measured by the morphometric analysis was comparable (56±2% versus 55±1%; P=NS) between MI+PBS (n=6) and MI+αGC (n=6) groups (Table 1).

Histomorphometric analysis of noninfarcted LV sections showed that myocyte cross-sectional area was increased in MI+PBS compared with sham mice and was significantly attenuated in MI+αGC (Figure 3A). Collagen volume fraction was also increased in MI+PBS compared with sham mice and was significantly attenuated in MI+αGC (Figure 3A).

There were rare TUNEL-positive nuclei in both sham and sham+αGC mice. The number of TUNEL-positive myocytes in the noninfarcted LV was increased in MI+PBS and was significantly decreased in MI+αGC (Figure 3B).

Myocardial MMP Activity

Representative gelatin zymography of the noninfarcted LV tissue at day 7 from 4 groups of mice was shown in Figure 4A. There were no zymographic MMP-2 and 9 levels in the sham+PBS and sham+αGC. Zymographic MMP-2 level was significantly increased in MI+PBS mice compared with sham mice at day 7. αGC injection significantly decreased this after MI (Figure 4B). Zymographic MMP-9 level was also increased in MI+PBS mice compared with sham mice at day 7, which, however, was not affected by αGC (Figure 4C).

Zymographic MMP-2 level was increased in MI+PBS mice also at day 28, and αGC injection tended to decrease it (3.7±1.1 versus 2.1±0.8 in ratio to sham, P=0.08).

Inflammatory and Cytokine Gene Expression

Immunohistochemical stainings for MAC3 and CD3 were increased in MI+PBS compared with sham+PBS and were further increased by αGC at day 7 (Figure 5). MPO-positive cells were not detected in the LV tissue from either group of mice (data not shown).

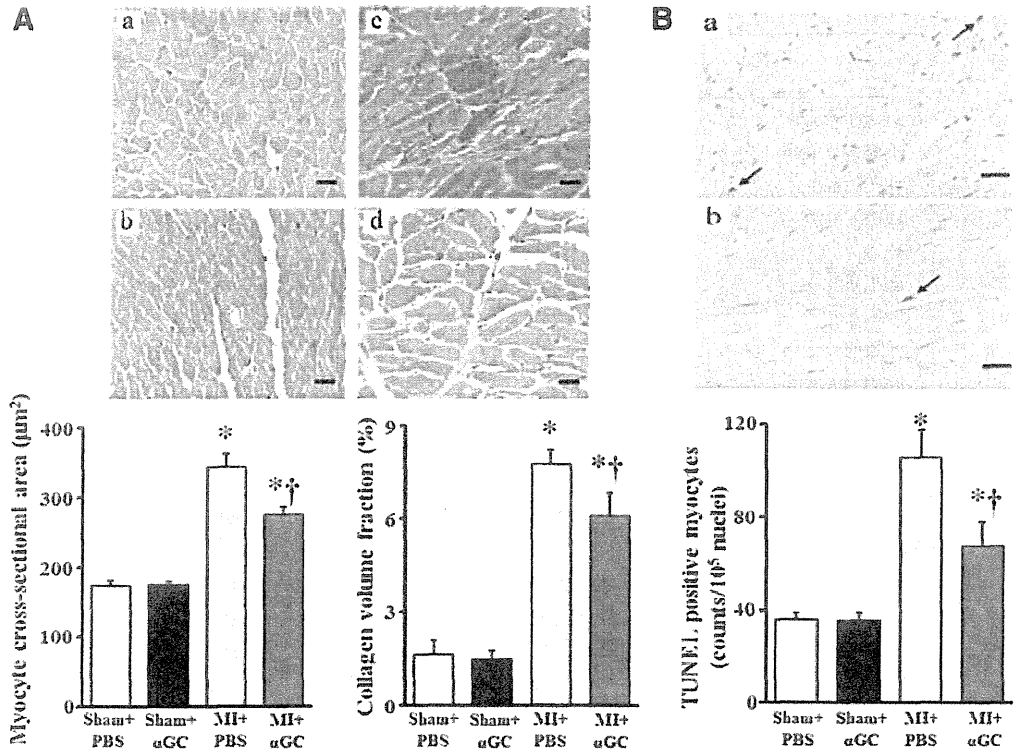

Figure 3. A, Representative high-power photomicrographs of LV cross sections stained with Masson trichrome from sham+PBS (a), sham+αGC (b), MI+PBS (c), and MI+αGC (d) and summary data of myocyte cross-sectional area and collagen volume fraction in 4 groups of mice (n=6). Scale bar, 20 μm. **B**, Representative photomicrographs TUNEL staining of LV sections from MI+PBS **(a)** and MI+αGC **(b)** and summary data for the number of TUNEL-positive cells in the noninfarcted LV (n=6). Scale bar, 20 μm. Data are expressed as mean±SEM. *P<0.05 versus sham+PBS, †P<0.05 versus MI+PBS.

CD11c (a marker of M1 macrophage) and arginase 1 (a marker of M2 macrophage) gene expressions were significantly increased in noninfarcted LV from MI+PBS compared with sham+PBS at day 7 (Figure 6A and 6B). αGC significantly increased their expressions in both sham and MI animals at day 7. Arginase 1 but not CD11c was increased in noninfarcted LV from MI+PBS and MI+αGC at day 28. There was no significant difference in arginase 1 between these 2 groups. MCP-1 and RANTES gene expressions were increased in noninfarcted LV from MI+PBS compared with sham+PBS at day 7 (Figure 6C and 6D). αGC significantly increased their expressions in both sham and MI animals at day 7. In contrast, there was no significant difference in their expressions among all groups at day 28.

IFN-γ, TNF-α, IL-6, and IL-10 gene expression levels were significantly increased in sham and MI mice by αGC at

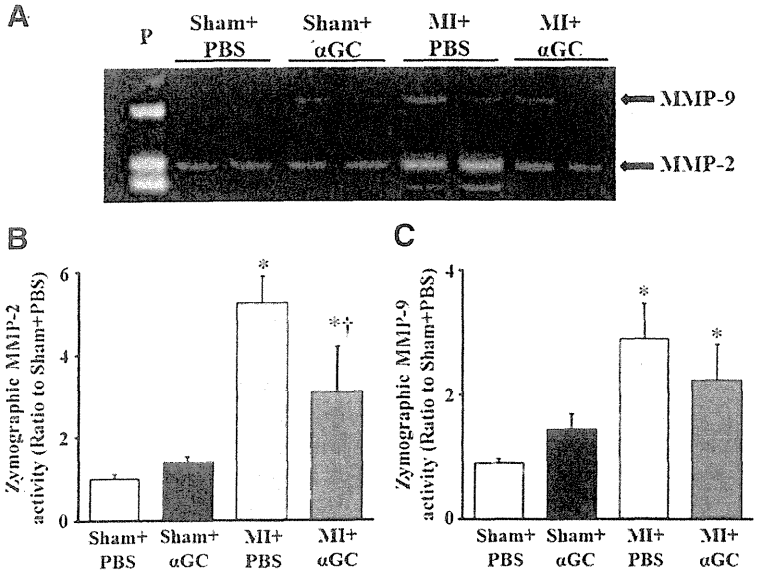

Figure 4. Representative LV zymographic MMP-2 and MMP-9 activities in noninfarcted LV at 7 days after surgery (A) and their densitometric analysis (B and C; n=5 for each). P indicates positive control. Data are expressed as mean±SEM. *P<0.05 versus sham+PBS, †P<0.05 versus MI+PBS.

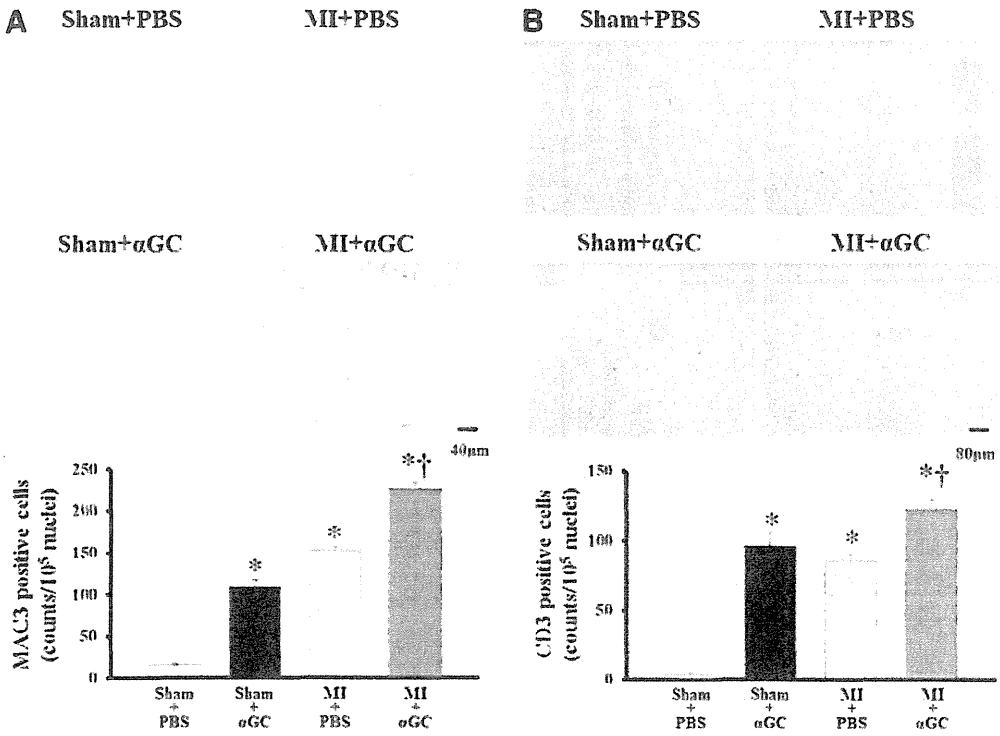

Figure 5. Representative photomicrographs of LV cross sections stained with (A, upper panel) anti-MAC3 and (B, upper panel), anti-CD3 in sham+PBS, sham+αGC, MI+PBS, and MI+αGC. Summary data of the numbers of **(A, lower panel)** MAC3 and **(B, lower panel)** CD3-positive cells in the LV (n=4–8 for each). Data are mean±SEM. *P<0.05 versus sham+PBS, †P<0.05 versus MI+PBS.

day 7 (Figure 6E through 6H). IL-10 gene expression alone significantly elevated up to 2.6-fold in the noninfarcted LV from MI+αGC mice at day 28 (Figure 6H). These time-dependent and αGC-mediated changes in IL-10 gene expression (Figure 6H) in the LV were matched with those in NKT cell infiltration (Figure 1B). IL-4 was not detected in either group.

Plasma Cytokine Concentration

Plasma IL-10 level was similar among sham+PBS, sham+αGC, and MI+PBS groups (9.0±0.5 versus 9.8±2.3 versus 10.6±2.3 pg/mL). However, in parallel to IL-10 gene expression in the LV, it significantly increased up to 2-fold in MI+αGC (21.1±2.3 pg/mL) compared with sham and MI+PBS mice (P<0.05). Plasma IFN-γ level was similar among 4 groups of mice (1.4±0.3 versus 1.7±0.3 versus 0.9±0.2 versus 1.0±0.2 pg/mL, P=NS). Plasma TNF-α, IL-6, and IL-4 levels were not detected in either group.

Experiment 3: Effects of IL-10 Neutralization on αGC-Treated Post-MI Heart Survival

The survival rate during 28 days tended to be higher in MI+αGC than in MI+anti–IL-10 receptor antibody and MI+αGC+anti–IL-10 receptor antibody (66.7% versus 44.4% and 42.1%, P=0.4).

Echocardiography and Hemodynamics

The echocardiographic and hemodynamic data from 3 groups of surviving mice are shown in Table 2. IL-10 receptor antibody injection significantly increased LV diameters, LVEDP, and decreased LV fractional shortening in αGC-treated MI mice. In contrast, there were no differences in these parameters between MI+anti–IL-10 receptor antibody and MI+αGC+anti–IL-10 receptor antibody. There was no significant difference in heart rate and aortic blood pressure among 3 groups.

Organ Weights and Infarct Size

In agreement with LVEDP, lung weight/body weight ratio was significantly increased in MI+αGC+anti–IL-10 receptor antibody compared with MI+αGC (Table 2). There were also no differences in these parameters between MI+anti–IL-10 receptor antibody and MI+αGC+anti–IL-10 receptor antibody.

Infarct size was comparable (56±2%, 54±2%, and 56±4%; P=NS) among MI+αGC (n=8), MI+anti–IL-10 antibody (n=8), and MI+αGC+anti–IL-10 receptor antibody (n=8) groups.

Experiment 4: Specificity of αGC for iNKT Cells

Immunohistochemical stainings for MAC3 and CD3 were increased in KO+MI+PBS compared with KO+sham+PBS. In contrast to the results from wild-type (Figure 5), αGC did not alter them (Online Figure I). MPO-positive cells were not detected in the LV tissue from either group of mice (data not shown). MCP-1 and RANTES were increased in KO+MI+PBS compared with KO+sham+PBS and were not affected by αGC (Online Figure IIA and B). There was

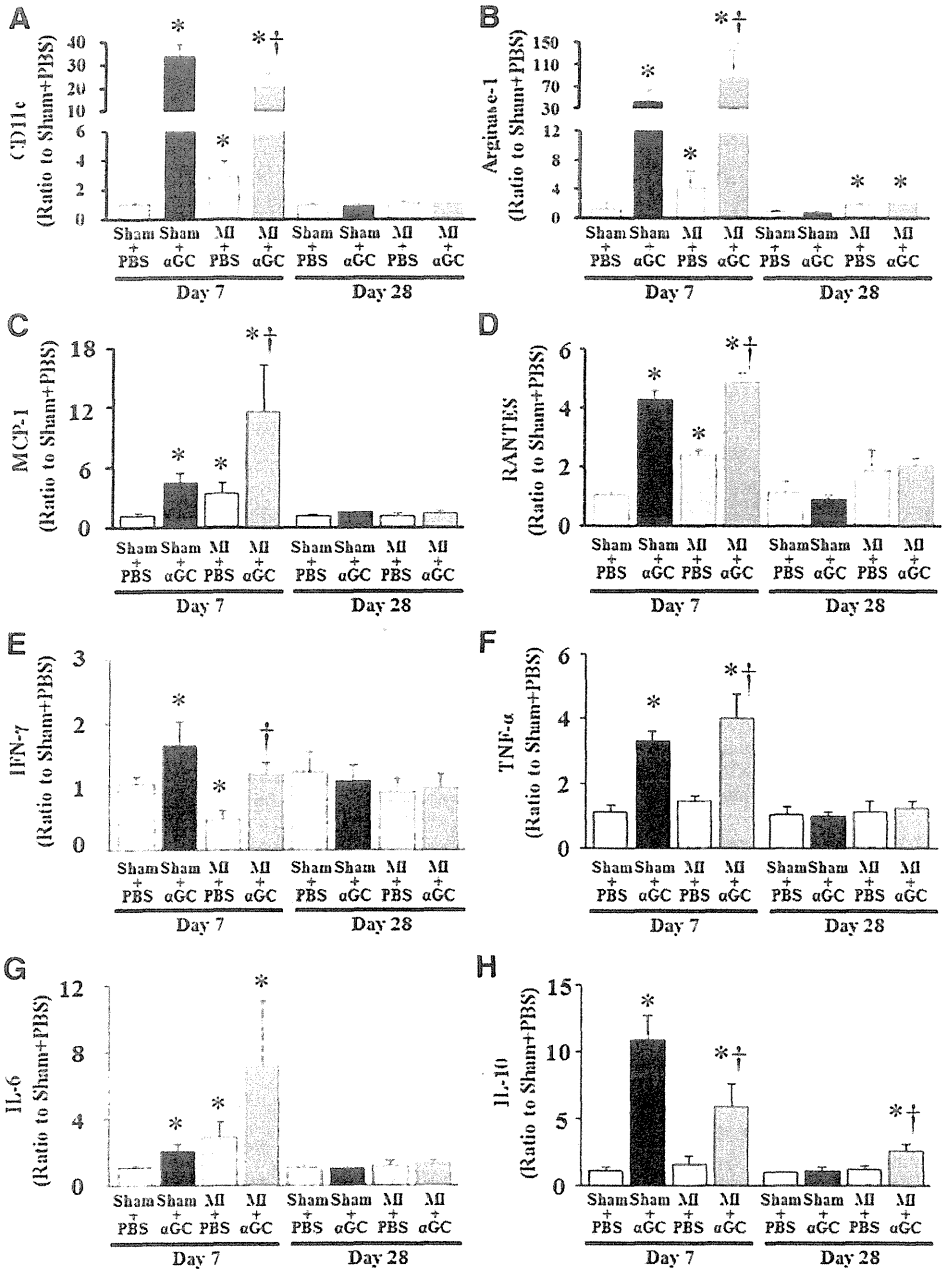

Figure 6. Quantitative analysis of gene expression of CD11c (A), arginase (B), MCP-1 (C), RANTES (D), IFN-γ (E), TNF-α (F), IL-6 (G), and IL-10 (H) in the noninfarcted LV at day 7 (n=6) and day 28 (n=4) after surgery. Gene expression was normalized to GAPDH and depicted as the ratio to sham+PBS. Data are expressed as mean±SEM. *P<0.05 versus sham+PBS, †P<0.05 versus MI+PBS.

no difference in TNF-α and IL-10 in the LV tissue from either group of mice (Online Figure IIC and D). These data suggest that αGC did not directly activate other inflammatory cell, induce chemokines, or produce inflammatory cytokines.

Discussion

The present study demonstrated that the activation of iNKT cells by αGC improved survival and ameliorated LV remodeling and failure after MI in mice, accompanied by the decreases in interstitial fibrosis, cardiomyocyte hypertrophy, and apoptosis. Furthermore, the enhanced expression of IL-10 by αGC is involved in these effects. This is the first report to provide direct evidence for increased iNKT cells in MI and the inhibitory effects of their activation on the development of post-MI HF.

Chronic Infiltration of Inflammatory Cells Including iNKT Cells in Post-MI Heart

In the setting of acute MI, the infiltration of inflammatory cells such as neutrophils, macrophages, and lymphocytes is a physiological repair process and beneficial removing dead cardiomyocytes and leading to the repair and scar formation of infarcted area.[18] However, the chronic inflammatory response in the noninfarcted area causes the further myocardial damage and fibrosis, leading to the progressive impairment of cardiac function.[19] We have previously demonstrated that anti–MCP-1 gene therapy improved survival and attenuated LV dilation and contractile dysfunction, which was associated with the decreases in macrophage infiltration and gene expression of myocardial inflammatory cytokines.[2] Therefore, chronic myocardial inflammation plays a crucial role on

Table 2. Echocardiography, Hemodynamics, and Organ Weights in Experiment 3

	MI+αGC (n=8)	MI+Anti–IL-10 Receptor Antibody (n=8)	MI+αGC+ Anti–IL-10 Receptor Antibody (n=8)
Echocardiography			
Heart rate, bpm	516±18	519±16	510±18
LVEDD, mm	4.8±0.1	5.4±0.1*	5.4±0.1*
LVESD, mm	3.9±0.1	4.6±0.1*	4.6±0.1*
FS, %	19±0.8	14.5±0.7*	15.4±0.7*
AWT, mm	0.30±0.01	0.37±0.06	0.35±0.06
PWT, mm	0.98±0.02	1.02±0.02	0.99±0.04
Hemodynamics			
Heart rate, min	518±16	487±17	515±22
Mean AoP, mm Hg	86±3	81±4	82±2
LVEDP, mm Hg	5.4±0.8	10.8±0.7*	11.4±3.3*
LV +dP/dt, mm Hg/s	10 441±661	6555±1031	7719±1284
LV –dP/dt, mm Hg/s	6847±569	4119±364	5774±1236
Organ weights			
Body wt, g	25.2±0.5	24.7±1.3	25.8±0.6
Heart wt/body wt, mg/g	6.3±0.3	8.8±0.9	6.9±0.5
Lung wt/body wt, mg/g	5.5±0.1	10.9±2.1*	7.9±1.0*
Infarct size, %	56±2	54±2	56±4

LVEDD indicates left ventricular end-diastolic diameter; LVESD, left ventricular end-systolic diameter; FS, fractional shortening; AWT, anterior wall thickness; PWT, posterior wall thickness; AoP, aortic pressure; LVEDP, left ventricular end-diastolic pressure; wt, weight. Data are mean±SEM.

*$P<0.05$ versus MI+ αGC.

LV remodeling and failure after MI. However, the precise role of various inflammatory cells and chemokines in this disease process has not been fully elucidated. iNKT cells are specialized lineage of T cells that recognize glycolipid antigens presented by the MHC class I–like molecule CD1d. The iNKT cells mediate various functions rapidly by producing a mixture of T_H1 and T_H2 cytokines and vast array of chemokines.[6] Thus, iNKT cells can function as a bridge between the innate and adaptive immune systems and orchestrate tissue inflammation. However, to our knowledge, there has been only one paper, by Olson et al, that reported the presence of iNKT cells in cardiac tissue obtained from acute Lyme carditis model.[20] Therefore, the present study was the first that demonstrated the increased infiltration of iNKT cells in post-MI hearts (Figure 1).

Effects of the Activation of iNKT Cells by αGC in Post-MI Heart

The most important finding of this study was that the activation of iNKT cells by αGC improved survival and attenuated LV remodeling and failure after MI (Figures 2 and 3 and Table 1). The beneficial effects of αGC were not attributable to its MI size-sparing effect, because the infarct size calculated as %LV circumference was comparable between MI+PBS and MI+αGC mice. Furthermore, its effects might not be attributable to those on hemodynamics, because blood pressure and heart rate were not altered (Table 1). αGC, a glycosphingolipid, is a well-known iNKT cell receptor ligand that can specifically activate iNKT cells.[13] It has been demonstrated that iNKT cells expand dramatically 2 to 3 days after in vivo treatment with αGC and return to the baseline level by approximately 9 days after treatment.[21,22] Moreover, the effects of iNKT cell stimulation may differ according to the timing of αGC administration. In the model of experimental autoimmune encephalomyelitis, early immunization with αGC protected against this disease, whereas later immunization potentiated it.[23] In the present study, αGC injection significantly enhanced iNKT cell infiltration (Figure 1) and could effectively ameliorate post-MI LV remodeling and failure (Figures 2 and 3).

Role of IL-10 in the Inhibitory Effects of iNKT Cell Activation by αGC

Another important finding of the present study was that the enhanced expression of IL-10 was involved in the inhibitory effects of iNKT cell activation against LV remodeling and failure (Table 2). These results are consistent with the previous findings that the therapeutic effects of αGC against T_H1-like autoimmune diseases include 2 mechanisms such as a shift from T_H1 toward a T_H2 pattern[9–11,23] and the induction of immunosuppressive cytokine IL-10.[9,11,12] The present study demonstrated that IL-10 was increased in noninfarcted LV from sham and MI animals in association with an increase in iNKT cells after the treatment with αGC at 7 days (Figure 6C and 6D). Interestingly, the enhanced expression of IL-10 gene by αGC persisted only in MI mice. These changes of IL-10 gene expression (Figure 6D) completely corresponded to those of iNKT cells (Figure 1B). Moreover, the inhibitory effects of αGC on LV remodeling and HF were reversed by anti–IL-10 receptor antibody and the treatment with only anti–IL-10 antibody of MI mice did not affect LV remodeling and HF (Table 2). Therefore, these data suggest that IL-10 is not associated with the development of LV remodeling and HF after MI without αGC, and IL-10 is involved in the beneficial effects of iNKT cell activation against post-MI remodeling and failure. These findings were consistent with a recent study by Krishnamurthy et al, in which LV dimension and function by echocardiography after MI did not differ between wild-type and IL-10–null mice.[24]

Possible Mechanisms of IL-10 for the Attenuation of LV Remodeling

IL-10 can inhibit the production of proinflammatory cytokines by macrophages and T_H1 cells[25,26] and directly promote the death of inflammatory cells.[27] Furthermore, beyond its suppressive effects on inflammatory gene synthesis, IL-10 also regulates extracellular matrix[28] and angiogenesis.[29] In the present study, the activation of iNKT cells by αGC decreased cardiac myocyte hypertrophy and apoptosis and inhibited interstitial fibrosis possibly through inhibiting the zymographic MMP-2 level in noninfarcted LV (Figure 4). MMP-2 is ubiquitously distributed in cardiac myocytes and fibroblasts and has been shown to play a crucial role in the

development of cardiac remodeling after MI.[30] Theoretically, an increase in MMP activity would result in a decrease in the MMP substrate, collagens, whereas an inhibition of MMP would result in an increase in collagens. However, our previous study showed that the selective disruption of the MMP-2 gene attenuated interstitial fibrosis after MI.[30] Therefore, the decrease in zymographic MMP-2 level by αGC might be involved in the attenuation of interstitial fibrosis in our model. On the other hand, MMP-9 is mainly expressed in infiltrating inflammatory cells such as neutrophils and T lymphocytes. A previous report showed that subcutaneous injection of recombinant IL-10 suppressed inflammation and attenuated LV remodeling after MI in mice by inhibiting fibrosis via suppression of HuR/MMP-9 and by enhancing capillary density through the activation of STAT3.[31] Moreover, the previous study by Burchfield et al showed that IL-10 from transplanted bone marrow mononuclear cells contributed to cardiac protection after MI in association with a decrease in T lymphocyte accumulation, reactive hypertrophy, and myocardial collagen deposition.[32] However, in the present study, zymographic MMP-9 level was not affected by αGC, which was consistent with the infiltration of lymphocyte observed by immunohistochemical staining for CD3 (Figure 5). We also measured the protein levels of HuR/MMP-9 or STAT3 in the noninfarcted LV. However, these protein levels were not affected by αGC (data not shown).

Role of Other Inflammatory Cells and Cytokines

In agreement with the increase in macrophage infiltration by αGC, MCP-1 gene expression was increased. αGC increased not only M1 macrophages but also M2 macrophages, which tune inflammatory responses and promote tissue repair.[33] Therefore, the increase in M2 macrophage might neutralize the effect of the increased M1 macrophage and MCP-1. The present study also showed that TNF-α was increased in noninfarcted LV from MI+αGC (Figure 6). TNF-α is a proinflammatory cytokine considered to be cardiotoxic and induce LV dysfunction.[34] However, in contrast, TNF-α has also protective effects during the maladaptive transition to HF.[35] Indeed, the treatment of patients with HF with either soluble TNF receptor (RENEWAL) or an anti-TNF antibody (ATTACH) could not show clinical benefits.[36,37] Therefore, the increase in TNF-α by αGC would not necessarily lead to the aggravation of LV remodeling.

Limitations

There are several limitations to be acknowledged in the present study. First, we could not directly demonstrate the location of iNKT cells by the immunohistochemical analysis using biotinylated CD1d dimer (BD Bioscience) with loading of αGC according to the previous report by Kamijyuku et al.[38] We tried the double immunohistochemical staining, using antibodies for anti–Armenian hamster TCR-β-PE (BD Bioscience) and anti-mouse NK 1.1-APC (BD Bioscience) according to the newly published paper.[39] Furthermore, we also performed in situ hybridization using digoxigenin-labeled DNA probes for mouse Vα14Jα18. Unfortunately, however, we could not detect iNKT cells in situ in the heart. Even though we defined iNKT cells within the heart by using the gene expression as well as the flow cytometric analysis, further studies are needed to overcome some technical difficulties of in situ detection and clarify this important issue. Second, the underlying mechanisms responsible for the activation of iNKT cells after MI remain to be established. To date, the endogenous ligand for iNKT cells has not been known. Based on our results using αGC, a glycosphingolipid, sphingolipid ceramide may be a crucial intermediate, since ceramide has been shown to be synthesized by long-chain fatty acids and actually increased in the heart after coronary microembolization.[40] Third, the source of IL-10 production after the stimulation of αGC remains to be determined. IL-10 has been shown to be produced by iNKT cells themselves on exogenous stimulation.[41] In addition, IL-10 can be expressed and secreted from macrophages activated by iNKT cells.[42,43] In the present study, the activation of iNKT cells by αGC injection increased the infiltration of macrophage in sham and MI mice at 7 days; however, there was no difference in it between MI+PBS and MI+αGC at 28 days (Figure 6). Therefore, the main source of IL-10 production at later phase of αGC injection would be the cells other than macrophages.

In conclusion, iNKT cells have a protective effect on LV remodeling and failure after MI via enhanced IL-10 expression. Therefore, therapies designed to activate iNKT cells may be beneficial against the development of post-MI heart failure.

Acknowledgments

We thank Kaoruko Kawai, Akiko Aita, and Miwako Fujii for excellent technical assistance.

Sources of Funding

This study was supported by grants from the Ministry of Education, Science, and Culture (17390223, 20590854, 20117004, 21390236) and Hokkaido Heart Association Grant for Research.

Disclosures

None.

References

1. Pfeffer MA, Braunwald E. Ventricular remodeling after myocardial infarction: experimental observations and clinical implications. *Circulation*. 1990;81:1161–1172.
2. Hayashidani S, Tsutsui H, Shiomi T, Ikeuchi M, Matsusaka H, Suematsu N, Wen J, Egashira K, Takeshita A. Anti-monocyte chemoattractant protein-1 gene therapy attenuates left ventricular remodeling and failure after experimental myocardial infarction. *Circulation*. 2003;108:2134–2140.
3. Varda-Bloom N, Leor J, Ohad DG, Hasin Y, Amar M, Fixler R, Battler A, Eldar M, Hasin D. Cytotoxic T lymphocytes are activated following myocardial infarction and can recognize and kill healthy myocytes in vitro. *J Mol Cell Cardiol*. 2000;32:2141–2149.
4. Shiomi T, Tsutsui H, Hayashidani S, Suematsu N, Ikeuchi M, Wen J, Ishibashi M, Kubota T, Egashira K, Takeshita A. Pioglitazone, a peroxisome proliferator-activated receptor-gamma agonist, attenuates left ventricular remodeling and failure after experimental myocardial infarction. *Circulation*. 2002;106:3126–3132.
5. Kaikita K, Hayasaki T, Okuma T, Kuziel WA, Ogawa H, Takeya M. Targeted deletion of CC chemokine receptor 2 attenuates left ventricular remodeling after experimental myocardial infarction. *Am J Pathol*. 2004;165:439–447.

6. Matsuda JL, Mallevaey T, Scott-Browne J, Gapin L. CD1d-restricted iNKT cells, the 'Swiss-Army knife' of the immune system. *Curr Opin Immunol.* 2008;20:358–368.
7. Nakai Y, Iwabuchi K, Fujii S, et al. Natural killer T cells accelerate atherogenesis in mice. *Blood.* 2004;104:2051–2059.
8. Ohmura K, Ishimori N, Ohmura Y, Tokuhara S, Nozawa A, Horii S, Andoh Y, Fujii S, Iwabuchi K, Onoe K, Tsutsui H. Natural killer T cells are involved in adipose tissues inflammation and glucose intolerance in diet-induced obese mice. *Arterioscler Thromb Vasc Biol.* 2010;30:193–199.
9. Hong S, Wilson MT, Serizawa I, Wu L, Singh N, Naidenko OV, Miura T, Haba T, Scherer DC, Wei J, Kronenberg M, Koezuka Y, Van Kaer L. The natural killer T-cell ligand alpha-galactosylceramide prevents autoimmune diabetes in non-obese diabetic mice. *Nat Med.* 2001;7:1052–1056.
10. Sharif S, Arreaza GA, Zucker P, et al. Activation of natural killer T cells by alpha-galactosylceramide treatment prevents the onset and recurrence of autoimmune Type 1 diabetes. *Nat Med.* 2001;7:1057–1062.
11. Furlan R, Bergami A, Cantarella D, Brambilla E, Taniguchi M, Dellabona P, Casorati G, Martino G. Activation of invariant NKT cells by alphaGalCer administration protects mice from MOG35–55-induced EAE: critical roles for administration route and IFN-gamma. *Eur J Immunol.* 2003;33:1830–1838.
12. Miellot A, Zhu R, Diem S, Boissier MC, Herbelin A, Bessis N. Activation of invariant NK T cells protects against experimental rheumatoid arthritis by an IL-10-dependent pathway. *Eur J Immunol.* 2005;35:3704–3713.
13. Van Kaer L. Alpha-galactosylceramide therapy for autoimmune diseases: prospects and obstacles. *Nat Rev Immunol.* 2005;5:31–42.
14. Kinugawa S, Tsutsui H, Hayashidani S, Ide T, Suematsu N, Satoh S, Utsumi H, Takeshita A. Treatment with dimethylthiourea prevents left ventricular remodeling and failure after experimental myocardial infarction in mice: role of oxidative stress. *Circ Res.* 2000;87:392–398.
15. Namba T, Tsutsui H, Tagawa H, Takahashi M, Saito K, Kozai T, Usui M, Imanaka-Yoshida K, Imaizumi T, Takeshita A. Regulation of fibrillar collagen gene expression and protein accumulation in volume-overloaded cardiac hypertrophy. *Circulation.* 1997;95:2448–2454.
16. Leuschner F, Panizzi P, Chico-Calero I, Lee WW, Ueno T, Cortez-Retamozo V, Waterman P, Gorbatov R, Marinelli B, Iwamoto Y, Chudnovskiy A, Figueiredo JL, Sosnovik DE, Pittet MJ, Swirski FK, Weissleder R, Nahrendorf M. Angiotensin-converting enzyme inhibition prevents the release of monocytes from their splenic reservoir in mice with myocardial infarction. *Circ Res.* 2010;107:1364–1373.
17. Kawano T, Cui J, Koezuka Y, Toura I, Kaneko Y, Motoki K, Ueno H, Nakagawa R, Sato H, Kondo E, Koseki H, Taniguchi M. CD1d-restricted and TCR-mediated activation of valpha14 NKT cells by glycosylceramides. *Science.* 1997;278:1626–1629.
18. Blankesteijn WM, Creemers E, Lutgens E, Cleutjens JP, Daemen MJ, Smits JF. Dynamics of cardiac wound healing following myocardial infarction: observations in genetically altered mice. *Acta Physiol Scand.* 2001;173:75–82.
19. Frangogiannis NG, Smith CW, Entman ML. The inflammatory response in myocardial infarction. *Cardiovasc Res.* 2002;53:31–47.
20. Olson CM Jr, Bates TC, Izadi H, Radolf JD, Huber SA, Boyson JE, Anguita J. Local production of IFN-gamma by invariant NKT cells modulates acute Lyme carditis. *J Immunol.* 2009;182:3728–3734.
21. Crowe NY, Uldrich AP, Kyparissoudis K, Hammond KJ, Hayakawa Y, Sidobre S, Keating R, Kronenberg M, Smyth MJ, Godfrey DI. Glycolipid antigen drives rapid expansion and sustained cytokine production by NK T cells. *J Immunol.* 2003;171:4020–4027.
22. Wilson MT, Johansson C, Olivares-Villagomez D, Singh AK, Stanic AK, Wang CR, Joyce S, Wick MJ, Van Kaer L. The response of natural killer T cells to glycolipid antigens is characterized by surface receptor down-modulation and expansion. *Proc Natl Acad Sci U S A.* 2003;100:10913–10918.
23. Jahng AW, Maricic I, Pedersen B, Burdin N, Naidenko O, Kronenberg M, Koezuka Y, Kumar V. Activation of natural killer T cells potentiates or prevents experimental autoimmune encephalomyelitis. *J Exp Med.* 2001;194:1789–1799.
24. Krishnamurthy P, Lambers E, Verma S, Thorne T, Qin G, Losordo DW, Kishore R. Myocardial knockdown of mRNA-stabilizing protein HuR attenuates post-MI inflammatory response and left ventricular dysfunction in IL-10-null mice. *FASEB J.*24:2484–2494.
25. Fiorentino DF, Zlotnik A, Vieira P, Mosmann TR, Howard M, Moore KW, O'Garra A. IL-10 acts on the antigen-presenting cell to inhibit cytokine production by Th1 cells. *J Immunol.* 1991;146:3444–3451.
26. Frangogiannis NG, Mendoza LH, Lindsey ML, Ballantyne CM, Michael LH, Smith CW, Entman ML. IL-10 is induced in the reperfused myocardium and may modulate the reaction to injury. *J Immunol.* 2000;165:2798–2808.
27. Wang P, Wu P, Siegel MI, Egan RW, Billah MM. Interleukin (IL)-10 inhibits nuclear factor kappa B (NF kappa B) activation in human monocytes. IL-10 and IL-4 suppress cytokine synthesis by different mechanisms. *J Biol Chem.* 1995;270:9558–9563.
28. Lacraz S, Nicod LP, Chicheportiche R, Welgus HG, Dayer JM. IL-10 inhibits metalloproteinase and stimulates TIMP-1 production in human mononuclear phagocytes. *J Clin Invest.* 1995;96:2304–2310.
29. Silvestre JS, Mallat Z, Duriez M, Tamarat R, Bureau MF, Scherman D, Duverger N, Branellec D, Tedgui A, Levy BI. Antiangiogenic effect of interleukin-10 in ischemia-induced angiogenesis in mice hindlimb. *Circ Res.* 2000;87:448–452.
30. Hayashidani S, Tsutsui H, Ikeuchi M, Shiomi T, Matsusaka H, Kubota T, Imanaka-Yoshida K, Itoh T, Takeshita A. Targeted deletion of MMP-2 attenuates early LV rupture and late remodeling after experimental myocardial infarction. *Am J Physiol Heart Circ Physiol.* 2003;285: H1229–H1235.
31. Krishnamurthy P, Rajasingh J, Lambers E, Qin G, Losordo DW, Kishore R. IL-10 inhibits inflammation and attenuates left ventricular remodeling after myocardial infarction via activation of STAT3 and suppression of HuR. *Circ Res.* 2009;104:e9–e18.
32. Burchfield JS, Iwasaki M, Koyanagi M, Urbich C, Rosenthal N, Zeiher AM, Dimmeler S. Interleukin-10 from transplanted bone marrow mononuclear cells contributes to cardiac protection after myocardial infarction. *Circ Res.* 2008;103:203–211.
33. Mantovani A, Sica A, Locati M. Macrophage polarization comes of age. *Immunity.* 2005;23:344–346.
34. Kubota T, McTiernan CF, Frye CS, Slawson SE, Lemster BH, Koretsky AP, Demetris AJ, Feldman AM. Dilated cardiomyopathy in transgenic mice with cardiac-specific overexpression of tumor necrosis factor-alpha. *Circ Res.* 1997;81:627–635.
35. Wang X, Oka T, Chow FL, Cooper SB, Odenbach J, Lopaschuk GD, Kassiri Z, Fernandez-Patron C. Tumor necrosis factor-alpha-converting enzyme is a key regulator of agonist-induced cardiac hypertrophy and fibrosis. *Hypertension.* 2009;54:575–582.
36. Mann DL, McMurray JJ, Packer M, et al. Targeted anticytokine therapy in patients with chronic heart failure: results of the Randomized Etanercept Worldwide Evaluation (RENEWAL). *Circulation.* 2004;109: 1594–1602.
37. Chung ES, Packer M, Lo KH, Fasanmade AA, Willerson JT. Randomized, double-blind, placebo-controlled, pilot trial of infliximab, a chimeric monoclonal antibody to tumor necrosis factor-alpha, in patients with moderate-to-severe heart failure: results of the anti-TNF Therapy Against Congestive Heart Failure (ATTACH) trial. *Circulation.* 2003;107: 3133–3140.
38. Kamijuku H, Nagata Y, Jiang X, et al. Mechanism of NKT cell activation by intranasal coadministration of alpha-galactosylceramide, which can induce cross-protection against influenza viruses. *Mucosal Immunol.* 2008;1:208–218.
39. Barral P, Sanchez-Nino MD, van Rooijen N, Cerundolo V, Batista FD. The location of splenic NKT cells favours their rapid activation by blood-borne antigen. *EMBO J.* 2012;31:2378–2390.
40. Thielmann M, Dorge H, Martin C, Belosjorow S, Schwanke U, van De Sand A, Konietzka I, Buchert A, Kruger A, Schulz R, Heusch G. Myocardial dysfunction with coronary microembolization: signal transduction through a sequence of nitric oxide, tumor necrosis factor-alpha, and sphingosine. *Circ Res.* 2002;90:807–813.
41. Sonoda KH, Faunce DE, Taniguchi M, Exley M, Balk S, Stein-Streilein J. NK T cell-derived IL-10 is essential for the differentiation of antigen-specific T regulatory cells in systemic tolerance. *J Immunol.* 2001;166:42–50.

42. Platzer C, Docke W, Volk H, Prosch S. Catecholamines trigger IL-10 release in acute systemic stress reaction by direct stimulation of its promoter/enhancer activity in monocytic cells. *J Neuroimmunol.* 2000;105:31–38.

43. Troidl C, Mollmann H, Nef H, Masseli F, Voss S, Szardien S, Willmer M, Rolf A, Rixe J, Troidl K, Kostin S, Hamm C, Elsasser A. Classically and alternatively activated macrophages contribute to tissue remodelling after myocardial infarction. *J Cell Mol Med.* 2009;13:3485–3496.

Novelty and Significance

What Is Known?

- Chronic tissue inflammation plays an important role in the development of left ventricular (LV) dysfunction and LV remodeling.
- Invariant natural killer T (iNKT) cells are a specialized lineage of T cells with NK marker. These cells produce a mixture of T_H1 and T_H2 cytokines and a vast array of chemokines to orchestrate tissue inflammation.
- iNKT cells play a protective role in experimental autoimmune and inflammatory diseases.

What New Information Does This Article Contribute?

- iNKT cells could be detected in normal heart, and their infiltration was increased in noninfarcted LV after myocardial infarction (MI).
- The activation of iNKT cells by α-galactosylceramide (αGC) improved survival and ameliorated LV remodeling and failure after MI in mice, accompanied by decreases in interstitial fibrosis, cardiomyocyte hypertrophy, and apoptosis.
- An increase in the expression of interleukin (IL)-10 by αGC was involved in the favorable effects for LV remodeling after MI.

iNKT cells regulate tissue inflammation by producing a mixture of T_H1 and T_H2 cytokines. Although chronic tissue inflammation is involved in the development of LV remodeling and failure, the pathophysiological role of iNKT cells in these processes have not been elucidated. Our study shows that infiltration of iNKT cells was increased in noninfarcted LV and their activation by αGC improved survival and ameliorated LV remodeling and failure after MI via enhanced expression of IL-10. These findings indicate a previously undescribed protective effect of iNKT cells on LV remodeling and failure after MI. Given that iNKT cells can bridge innate and adaptive immune systems, they could act as an upstream regulator of cytokine networks in the heart. Therapies designed to regulate iNKT cells and to modulate cytokine network may be beneficial in ameliorating LV remodeling and failure.

Supplemental Material

Detailed Methods

An expanded Methods section is available in the online Data Supplement at http://circres.ahajournals.org.

All procedures and animal care were approved by our institutional animal research committee and conformed to the animal care guideline for the Care and Use of Laboratory Animals in Hokkaido University Graduate School of Medicine.

Experiment 1: Time-dependent Changes of iNKT Cell Receptors in Post-MI Hearts

Animal Models

MI was created in male C57BL/6J mice, 6-8 weeks old and 20 to 25 g body weight, by ligating the left coronary artery as described previously.[1] Sham operation without ligating the coronary artery was also performed as control. MI mice were sacrificed and the hearts were excised at day 3, 7, 14 and 28 for quantitative reverse transcriptase (qRT)-PCR measurements.

Quantitative Reverse Transcriptase PCR

Total RNA was extracted from LV in sham mice and non-infarcted and infarcted LV from MI mice by using QuickGene-810 (FujiFilm, Tokyo, Japan) according to the manufacturer's instructions. cDNA was synthesized with the high capacity cDNA reverse transcription kit (Applied Biosystems, Foster City, CA). TaqMan quantitative PCR was performed with the 7300 real-time PCR system (Applied Biosystems) to amplify samples for Vα14Jα18 (a specific marker of iNKT cells).[2] This transcript was normalized to GAPDH. The primer was purchased from Applied Biosystems.

Experiment 2: Effects of iNKT Cell Activation on Post-MI Hearts

Animal Models

Sham and MI mice were created in male C57BL/6J as described in Experiment 1. Each group of mice was randomly divided into 2 groups; either α-galactosylceramide (αGC; 0.1μg/g body weight; Funakoshi Company, Ltd., Tokyo, Japan), the activator of iNKT cells, or phosphate-buffered saline (PBS) was administered via intraperitoneal injection 1 and 4 days after surgery. The concentration of αGC was chosen based on the previous study of its efficacy.[2] Thus, the experiment was performed in the following 4 groups of mice; sham+PBS (n=10), sham+αGC (n=10), MI+PBS (n=31), and MI+αGC (n=27).

Four weeks after surgery, echocardiographic studies and the hemodynamics measurement were performed. After collecting blood samples, mice were sacrificed and organ weight was measured. These measurements were performed in all survived mice (n=10 for sham+PBS, n=10 for sham+αGC, n=10 for MI+PBS, and n=16 for MI+αGC). The mice were further divided into 2 groups; for the histological analysis, including infarct size, myocyte cross-sectional area, collagen volume fraction, TUNEL staining (n=6 for each group), and for the quantitative reverse transcriptase PCR (n=4 for

each group). Additional mice were also created for MMP zymography (n=5 for each group) and for flow cytometry analysis (n=9 for each group).

A separate group of additional mice treated identically was created. One week after surgery, all mice (n=15 for each group) were sacrificed. These mice were used for immunohistochemistry (n=3 for each group), for the quantitative reverse transcriptase PCR (n=6 for each group), and for flow cytometry (n=9 for each group).

Survival

The survival analysis was performed in all 4 groups of mice. During the study period, the cages were inspected daily for deceased animals. All deceased mice were examined for the presence of MI as well as pleural effusion and cardiac rupture.

Echocardiographic and Hemodynamic Measurements

Echocardiographic and hemodynamic measurements were performed under light anesthesia with tribromoethanol/amylene hydrate (avertin; 2.5% wt/vol, 8 μL/g ip) with known short duration of action and modest cardiodepressive effects. A two-dimensional parasternal short-axis view was obtained at the levels of the papillary muscles. In general, the best views obtained with the transducer lightly applied to the mid upper left anterior chest wall. The transducer was then gently moved cephalad or caudad and angulated until desirable images were obtained. After it had been ensured that the imaging was on the axis, two-dimensional targeted M-mode tracings were recorded at a paper speed of 50mm/s. A 1.4-Fr micromanometer-tipped catheter (Millar Instruments, Houston, Texas) was inserted into the right carotid artery and then advanced into the left ventricle (LV) to measure LV pressures.

Myocardial Histopathology and Infarct Size

After mice were sacrificed, the heart was excised and dissected into right ventricle and LV including septum. LV was cut into three transverse sections; apex, middle ring, and base. From the middle ring, 5-μm sections were cut and stained with Masson's trichrome. Myocyte cross-sectional area and collagen volume fraction were determined by quantitative morphometry of tissue sections from the mid-LV as described previously.[3]

Infarct length was measured along the endocardial and epicardial surfaces in each of the cardiac sections, and the values from all specimens were summed. Infarct size (as a percentage) was calculated as total infarct circumference divided by total cardiac circumference.[1]

Myocardial Apoptosis

To detect apoptosis, tissue sections from the mid-LV were stained with the terminal deoxynucleotidyl transferase-mediated dUTP nick end-labeling (TUNEL) staining (TaKaRa Shuzo Co. Ltd., Ohtsu, Japan). The number of TUNEL positive cardiac myocyte nuclei was counted, and the data were normalized per 10^5 total nuclei identified by hematoxylin-positive staining in the same sections. The proportion of apoptotic cells was counted in the non-infarcted LV.

MMP Zymography

Zymographic MMP 2 and 9 levels in LV non-infarcted tissue was determined using gelatin zymography kit (Primary Cell Co., Ltd, Sapporo, Japan). The zymograms were digitized, and the size-fractionated bands, which indicated proteolytic levels, were measured by the integrated optical density in a rectangular region of interest.[1]

Isolation of Cardiac Mononuclear Cell and Flow Cytometry

LV tissue was harvested, minced with a fine scissors, placed in 10 ml RPMI-1640 with 5% FBS, 1 mg/ml collagenase type IV and 100 U/ml DNase I, and shaken at 37 °C for 45 min. Tissue was then triturated through nylon mesh and centrifuged (1400 rpm, 5min, 4 °C). Red blood cells were lysed with Tris-NH_4Cl solution. Cardiac mononuclear cells were isolated by density-gradient centrifugation with 33% Percoll™, as previously described.[4] Cardiac mononuclear cells from 3 mice were pooled, and subjected to flow cytometric analysis. All reagents were purchased from Sigma-Aldrich (St Louis, MO). Cardiac cell numbers were determined with Trypan blue (Wako Pure Chemical Industries, Ltd., Osaka, Japan).

The cells were incubated with 2.4G2 monoclonal antibody (mAb) to block non-specific binding of primary mAb and then reacted with Dimer X (CD1d:Ig recombinant fusion protein; BD Biosciences Pharmingen, San Diego, CA) loaded with αGC, followed by detection with phycoerythrin (PE)-conjugated anti-mouse IgG1 mAb (BD) according to the manufacturer's protocol.[5] After washing, cells were stained with a combination of fluorescein isothiocyanate (FITC)-anti-TCRβ and PE-anti-mouse IgG1 (all from BD Biosciences). Stained cells were acquired with FACS Canto II flow cytometer (BD Biosciences Immunocytometry Systems, San Jose, CA) and analyzed with FlowJo (Tommy Digital Biology, Tokyo, Japan). Propidium iodide (Sigma-Aldrich, St Louis, MO) positive cells were electronically gated as dead cells from the analysis.

RT-PCR

RNA was extracted and cDNA was synthesized were described in Experiment 1. TaqMan quantitative PCR was performed with the 7300 real-time PCR system (Applied Biosystems) to amplify samples for Vα14Jα18, CD11c (a marker of M1 macrophages), arginase-1 (a marker of M2 macrophages), MCP-1, RANTES, interferon-γ (IFN-γ), IL-4, IL-6, TNF-α, and IL-10 cDNA. These transcripts were normalized to GAPDH.

Immunohistochemistry

LV sections were immunostained with antibody against mouse MAC3 (a macrophage marker), mouse CD3 (a T cell marker), or mouse myeloperoxidase (a leucocyte marker), followed by counter-staining with hematoxylin.

Plasma Cytokines Concentration

Plasma IL-10, TNF-α, IFN-γ, IL-6, and IL-4 levels were measured by commercially